Journal of Pharmaceutical Analysis 14 (2024) 100927

Contents lists available at ScienceDirect

Journal of Pharmaceutical Analysis

journal homepage: www.elsevier.com/locate/jpa

Original article

Cornus officinalis with high pressure wine steaming enhanced anti-hepatic fibrosis: Possible through SIRT3-AMPK axis

Xin Han [1], Yan Ning [1], Xinyue Dou [1], Yiwen Wang [1], Qiyuan Shan, Kao Shi, Zeping Wang, Chuan Ding, Min Hao, Kuilong Wang, Mengyun Peng, Haodan Kuang, Qiao Yang, Xianan Sang**, Gang Cao*

School of Pharmacy, Zhejiang Chinese Medical University, Hangzhou, China

ARTICLE INFO

Article history:
Received 21 September 2023
Received in revised form
7 December 2023
Accepted 19 December 2023
Available online 21 December 2023

Keywords:
Liver fibrosis
SIRT3
Cornus officinalis
AMPK
Caspase6

ABSTRACT

Cornus officinalis, a medicinal and edible plant known for its liver-nourishing properties, has shown promise in inhibiting the activation of hepatic stellate cells (HSCs), crucial indicators of hepatic fibrosis, especially when processed by high pressure wine steaming (HPWS). Herein, this study aims to investigate the regulatory effects of *cornus officinalis*, both in its raw and HPWS forms, on inflammation and apoptosis in liver fibrosis and their underlying mechanisms. *In vivo* liver fibrosis models were established by subcutaneous injection of CCl_4, while *in vitro* HSCs were exposed to transforming growth factor-β (TGF-β). These findings demonstrated that *cornus officinalis* with HPWS conspicuously ameliorated histopathological injury, reduced the release of proinflammatory factors, and decreased collagen deposition in CCl_4-induced rats compared to its raw form. Utilizing ultra-high-performance liquid chromatography coupled with quadrupole time-of-flight mass spectrometer (UHPLC-QTOF-MS) combined with network analysis, we identified that the pharmacological effects of the changed components of *cornus officinalis* before and after HPWS, primarily centered on the adenosine phosphate (AMP)-activated protein kinase (AMPK) pathway. Of note, *cornus officinalis* activated AMPK and Sirtuin 3 (SIRT3), promoting the apoptosis of activated HSCs through the caspase cascade by regulating caspase3, caspase6 and caspase9. siRNA experiments showed that *cornus officinalis* could regulate AMPK activity and its mediated-apoptosis through SIRT3. In conclusion, *cornus officinalis* exhibited the ability to reduce inflammation and apoptosis, with the SIRT3-AMPK signaling pathway identified as a potential mechanism underlying the synergistic effect of *cornus officinalis* with HPWS on anti-liver fibrosis.

1. Introduction

Liver fibrosis characterized by extracellular matrix (ECM) deposition, is a consequence of various chronic liver injuries, including viral hepatitis, nonalcoholic steatohepatitis (NASH), and alcoholic fatty liver (ALD) [1]. Without treatments, liver fibrosis can progress to cirrhosis and even hepatocellular carcinoma, posing a significant threat to human health [2]. Despite more than four decades of steady progress toward exploring the mechanism and clinical outcomes of liver fibrosis, the approval of effective anti-fibrosis drugs by the Food and Drug Administration (FDA) has been limited [3]. Nevertheless, recent research has shown that Traditional Chinese Medicine (TCM) offers unique advantages in the treatment of fibrosis [4–7]. *Cornus officinalis*, the dried fruit of *Cornus officinalis* Sieb. et Zucc, is classified as an edible and herbal plant in TCM and has a historical use in nourishing the liver and kidney [8]. Modern pharmacological studies have shown that *cornus officinalis* extract could reduce the level of inducible nitric oxide synthase and cyclooxygenase-2, as well as inhibit nuclear ectopia of nuclear factor kappa-B (NF-κB) in macrophages [9], indicating that *cornus officinalis* had anti-inflammatory and anti-oxidant effects. In addition, processed *cornus officinalis* can ameliorate NASH through reducing body weight and improving hepatic steatosis [10]. With further research, the material basis of the pharmacological effect of *cornus officinalis* was revealed, that is, its active ingredients [8]. To date, over 300 compounds have been

* Corresponding author.
** Corresponding author.
E-mail addresses: sangxianan@zcmu.edu.cn (X. Sang), caog1984@zcmu.edu.cn (G. Cao).
[1] These authors contributed equally to this work.

https://doi.org/10.1016/j.jpha.2023.12.017

isolated and identified from *cornus officinalis*, including flavones, terpenes, polysaccharides, and more [8,11]. Among these, quercetin is a flavone from *cornus officinalis* and can inhibit macrophage pyroptosis induced by oxidative stress through Adenosine monophosphate-activated protein kinase (AMPK) pathway [12,13]. Notably, morroniside (MO), a secoiridoid glycoside, is a main component in *cornus officinalis* and attenuates apoptosis and the inflammatory response by inhibiting NF-κB signaling [14]. Moreover, morroniside exerts an anti-fibrotic effect by inhibiting the activation of hepatic stellate cells (HSCs) [15]. Therefore, *cornus officinalis* has a certain liver protective effect, which may be related to inflammation and HSCs cell activation.

In liver fibrosis, activated HSCs with contractile and proliferative features become myofibroblast-like cells, expressing α-smooth muscle actin (α-SMA) and collagen, components of the ECM [16,17]. Recent studies have shown that early liver fibrosis can be reversed once the injury ceases, with approximately half of activated HSCs returning to an inactive state via apoptosis or deactivation [18]. Our previous study showed that *cornus officinalis* could inhibit the activation of HSCs, and its high pressure wine steaming (HPWS) products has a superior inhibitory effect [19]. Consistently, it is reported that the regulatory effects on the pharmacology of *cornus officinalis* differ between the were raw and post-processed [20]. These findings provide sufficient scientific evidence for the utilization of *cornus officinalis* in the prevention and treatment of liver fibrosis, although the specific mechanism remains unclear. A study showed that *cornus officinalis* can regulate cell apoptosis through the AMPK pathway [21] that a key hub for energy perception and metabolic regulation [22]. Compelling evidence has shown that the downregulation of AMPK results in the persistent activation of caspase-6, facilitating hepatocyte damage and even death, accompanied by the releases of damage-associated molecular patterns (DAMPs) that activated HSCs [23]. Recent studies have shown that Sirtuin 3 (SIRT3) overexpression can activate the AMPK signaling pathway, which is essential for improving biogenesis and suppressing apoptosis in mitochondrial [24]. Under normal conditions, SIRT3 can bind to adenosine triphosphate (ATP) synthase and participate in the conversion of orthophosphate and adenosine diphosphate into ATP, thereby altering the activity of AMPK [25,26]. SIRT3, which is located in mitochondrial inner membrane, is an NAD-dependent deacetylation protein and plays a vital role in oxidative stress [27], energy homeostasis [28], inflammation [29] and apoptosis. It's worth mentioning is that overexpression of SIRT3 can ameliorate the lipid toxicity of hepatocytes by activating AMPK [30]. However, whether *cornus officinalis* with HPWS can regulate AMPK and its mediated apoptosis through SIRT3 in liver fibrosis, is the question to be addressed in this study.

Therefore, techniques such as gene knockout were used to explore the anti-fibrosis effect and its mechanism, combined with network pharmacology and ultra-high-performance liquid chromatography coupled with quadrupole time-of-flight mass spectrometer (UHPLC-QTOF-MS) to identify the active ingredients of *cornus officinalis* in the anti-fibrosis properties. This research aims to lay the foundation for elucidating the scientific significance of enhancing the efficiency of Chinese medicine processing efficiency enhancement.

2. Materials and methods

2.1. Plant material

Cornus officinalis was obtained from Pan'an City of Zhejiang Province and authenticated by Prof. Bo Zhu and Kaohua Liu. The preparations of *cornus officinalis* with or without HPWS according to the experimental conditions as described earlier [19]. In brief, a certain amount of *cornus officinalis* samples was braised with rice wine dosage (*m*/*m*) at 25% for 1 h, following steamed at 115 °C for 1 h, and dried at 60 °C, finally the *cornus officinalis* with HPWS were obtained. For animal and cell treatment, *cornus officinalis* with raw and HPWS were crushed and sifted via 2-size screen (850 ± 29 μm), refluxed with 90% and 50% ethanol. The filtrates were collected and transformed into freeze-dried powder through vacuum concentration and lyophilization.

2.2. Chemical reagents

Anti-α-SMA (cs19245), anti-p-AMPKα (cs2535), anti-caspase-1 (cs24232) and anti-NOD-like receptor thermal protein domain associated protein 3 (NLRP3) (cs15101) were purchased from Cell Signaling Technology (Danvers, MA, USA). Anti-CollagenI (ab34710), anti-Tissue Inhibitors of Metalloproteinase 1 (TIMP1) (ab61224), anti-caspase-3 (ab179517), anti-beclin-1 (ab210498), anti-Bcl-2 (ab194583) antibodies and the horseradish peroxidase (HRP)-conjugated goat anti-rabbit (ab97051) were purchased from Abcam (Cambridge, MA, USA). Anti-CollagenI (14695-1-AP), anti-SIRT3 (10099-1-AP), anti-F4/80 (28463-1-AP), anti-caspase-6 (10198-1-AP), anti-caspase-9 (10380-1-AP) and anti-GAPDH (60004-1-Ig) antibodies were purchased from Proteintech (Wuhan, HubChina). Anti-Matrix metalloproteinase-13 (MMP-13) (sc515284) and anti-Interleukin (IL)-1R1 (sc393998) antibodies were purchased from Santa Cruz Biotechnology (Stanta Cruze, CA, USA). Anti-IL-1β (mab4012) antibodies were purchased from R&D Systems (Minneapolis, MN, USA). Alexa Fluor 488 Goat anti-Mouse IgG (A11034) and Alexa Fluor Plus 647 Goat anti-Rabbit IgG (A32727) were purchased from Beyotime Biotechnology (Shanghai, China).

2.3. Animals experiments

Male adult Sprague-Dawley rats weighing 200 ± 20 g (the certificate number: SCXK [Shanghai] 2017-0005) were obtained from Shanghai Slac Laboratory Animal Co., Ltd. (Shanghai, China). All animals were acclimatized in an air-conditioned animal center with a 12 h light/dark cycle for a week. They also had freely access to food and water in 60% relative humidity at 25 °C. All animal experiments were approved by the Animal Experimental Ethics Committee of Zhejiang Chinese Medicine University (Approval number: 47360).

The rats were divided randomly into seven groups (10 rats per group): control group, CCl_4 group, CCl_4 plus *cornus officinalis* with or without HPWS group (0.3 g/kg, 1 g/kg), CCl_4 plus the colchicine (0.2 mg/kg) group. And colchicine was considered as a positive control. Except for the control group, rat in other groups were subcutaneously injected with 40% CCl_4 in olive oil (6 mL/kg) once in the first week, and 40% CCl_4 in olive oil (3 mL/kg) for the subsequent seven weeks at twice per week. Rats in the *cornus officinalis* groups and colchicine group were administered by oral gavage with *cornus officinalis* with or without HPWS (0.3 g/kg, 1 g/kg) or colchicine (0.2 mg/kg) for eight weeks, respectively. The control group was given the same dose of saline. Rats were sacrificed with anesthesia used 3% sodium pentobarbital after eight weeks. Following the abdomen of the rats was opened rapidly, and blood were collected from the abdominal aorta, whereafter liver samples were collected and stored at −80 °C.

2.4. Serum biochemical analysis

Serum alanine aminotransferase (ALT) and aspartate aminotransferase (AST) were measured with automatic biochemical analyzer from Hitachi Ltd. (Tokyo, Japan).

2.5. Histological analysis

The liver tissues were embedded with Tissue-Tek® O.C.T. Compound (Torrance, CA, United States) and made into frozen sections. After fixation with methanol and acetone mixture, the sections were stained with hematoxylin and eosin (H&E) solution, Sirius Red solution and Masson's Trichrome Stain Kit from Solarbio Science & Technology Co., Ltd. (Beijing, China) according to the manufacturer's instructions.

2.6. Analysis of components in cornus officinalis

The powder of approximately 1.0 g *cornus officinalis* (both raw and HPWS) were dissolved in 25 mL 80% methanol, separately. All solutions were filtered with a 0.22 μm microfiltration membrane and samples were obtained. For component analysis, all samples were analyzed using a UPLC-HRMS method. Chromatography separation was performed by using acquity I-class ultra-high performance liquid chromatography system and a Waters HSS T3 column (100 mm × 2.1 mm, 1.8 μm) (Milford, MA, USA). The mobile phase: A was consisted of 0.1% (*V/V*) aqueous formic acid, B was acetonitrile containing 0.1% (*V/V*) formic acid. Gradient elution: 0–2 min, 98–95% A; 2–10 min, 95–85% A; 10–15 min, 85–75% A; 15–18 min, 75–50% A; 18–23 min, 50–0% A; 23–25 min, 0–98% A; 25–30 min, 98% A. The flow rate was 0.3 mL/min, the injection volume was 1 μL and column temperature was 30 °C. Mass spectrometric analysis was performed by the Xevo G2-XS QTOF mass spectrometer instrument equipped with an Zspra™ ESI source from Waters (Milford, MA, USA) that operated in negative ionization mode. Mass spectra were acquired in negative ionization mode using data-dependent acquisition (DDA) mode with a mass range of *m/z* 50–2,000. The mass spectrometry conditions were set as follows: ESI source temperature, 100 °C; de-solvation temperature, 500 °C; a spray voltage, 3.5 kV; a cone gas flow rate, 100 L/h; and a desolvation gas flow rate, 1,000 L/h. Data were acquired in centroid format. Masslynx software was used for raw mass spectrometry data processing and quantitative analyses from Waters.

2.7. Prediction of potential targets of differential compounds

Information on the targets of the differential compounds in *cornus officinalis* between raw and HPWS was collected from the Traditional Chinese Medicine Systems Pharmacology Database and Analysis Platform (TCMSP) (https://old.tcmsp-e.com/tcmsp.php), the Encyclopedia of Traditional Chinese Medicine database (ETCM) (http://www.tcmip.cn/ETCM/index.php/Home/Index/), Bioinformatics Analysis Tool for Molecular mechanism of Traditional Chinese Medicine database (BATMAN-TCM) (http://bionet.ncpsb.org.cn/batman-tcm/), SymMap database (http://www.symmap.org/), SwissTargetPrediction database (http://swisstargetprediction.ch/) and TargetNet database. Similarly, disease related targets were collected from three databases using 'liver fibrosis' as the keyword: the GeneCards database (https://www.genecards.org/), the Online Mendelian Inheritance in Man (OMIM) database (https://www.omim.org/) and the Disease Gene Network (DisGeNET) (https://www.disgenet.org/). The candidate targets of differential compounds and therapeutic targets of liver fibrosis were imported into VENNY2.1 (https://bioinfogp.cnb.csic.es/tools/venny/) for visualized and intersected to obtain potential targets for *cornus officinalis* treatment liver fibrosis. Finally, the potential targets were performed for the Kyoto Encyclopedia of Genes and Genomes (KEGG) signaling pathway using Metascape platform (http://metascape.org/). A value of P <0.05 was used to identify key KEGG pathways. The top-ranked results of KEGG enrichment analyses were screened and visualized using bioinformatics platform (http://www.bioinformatics.com.cn/).

2.8. Cell culture and treatments

Rat HSCs line HSC-T6 was purchased from Procell Life Science & Technology Co., Ltd (Wuhan, China) and cultured in DMEM supplemented with 10% fetal bovine serum, 100 U/mL penicillin and 100 μg/mL streptomycin at 37 °C under 5% CO_2. For MTT assay, HSC-T6 cells were cultured in 96-well plates and exposed to *cornus officinalis* (0–1,000 μg/mL) with or without TGF-β (10 ng/mL). The establishment of liver fibrosis model *in vitro* was referred to the previous experimental [31]. To be specific, cells cultured in 6-well plates were treated with TGF-β (10 ng/mL) *Cornus officinalis* with or without HPWS (50, 250 μg/mL) for 24 h. The cells were collected for follow-up experiments.

2.9. Transfection of HSC-T6 cells with lentivirus-mediated RNAi

The knockdown of SIRT3 were conducted using lentivirus-mediated RNAi according to the manufacturer's protocols. To be specific, logarithmic HSC-T6 cells were cultured in a 6-well plate at a number of 5×10^5 per hole. For transfection, cells at the confluence of 20–30% were treated with HitransG P and lentivirus-mediated SIRT3 RNAi (sequence: 5′-GCCCAATGTCGCTCACTACTT-3′) obtained from GeneChem for 72 h. Subsequently, the cells were screened with puromycin at 4 μg/mL for 48 h and then collected for identification, finally stable cell lines with knockdown of SIRT3 were obtained and used for follow-up experiment.

2.10. Western blotting analysis

Total proteins were extracted from liver tissues and HSC-T6 using lysis buffer from Solarbio Science & Technology Co., Ltd. (Beijing, China) supplemented with phosphatase and protease inhibitors, and protein concentrations were measured by BCA protein assay kit. Equivalent proteins were separated by sodium dodecyl sulfate-polyacrylamide gel electrophoresis (SDS-PAGE) and then transferred to polyvinylidene fluoride (PVDF) membranes. Membranes were blocked with 5% skim milk that was dissolved in phosphate buffered saline containing 0.05% tween 20 for 1 h at room temperature and then incubated with specific primary antibodies at 4 °C overnight. Thereafter, the membranes were washed and incubated with respective HRP-conjugated secondary antibodies for 1 h at room temperature. After washed, the membranes were detected with enhanced chemiluminescence from Beyotime Biotechnology (Shanghai, China) and photographed using ProteinSimple imaging system (Sanfrancisco, CA, USA). The bands were analyzed by Quantity One software obtained from Bio-Rad Laboratories Inc., (Hercules, CA, USA).

2.11. Immunofluorescence staining

Cryosections and cells were fixed with acetone and methanol mixture or 4% paraformaldehyde, respectively, incubated with 5% goat serum for 0.5 h at room temperature to reduce non-specific binding. Subsequently, liver sections and cells were incubated with primary antibodies overnight at 4 °C, followed stained with Alexa Fluor 488 Goat anti-Mouse IgG (A11034) or Alexa Fluor Plus 647 Goat anti-Rabbit IgG (A32727). Finally, the nuclei were stained

with DAPI. The fluorescence was visualized by a Zeiss orthographic fluorescence microscope in a blinded manner.

2.12. Apoptosis detection using flow cytometry

Apoptosis of HSC-T6 cells was detected by Annexin V-FITC/PI Apoptosis Detection kit Lianke Biotechnology (Hangzhou, China) according to the manufacturer's instructions. The HSC-T6 cells were digested into single cells using Accutase. After stimulation, 1.0×10^6 HSC-T6 cells were washed with cold PBS and resuspended in binding buffer. Then, Annexin V-FITC and propidium iodide (PI) staining was performed in the dark at room temperature for 5 min. Apoptotic cells were detected by flow cytometry using a BD LSRFortessa SORP (Franklin Lakes, NJ, USA) and were analyzed with CytExpert analytical software.

2.13. Statistical analysis

All data were presented as the mean ± SD. One-way ANOVA statistical test was used for the analysis of comparisons. All analysis were performed by using GraphPad Prism (San Diego, CA, USA). Statistically significant differences between groups were defined as

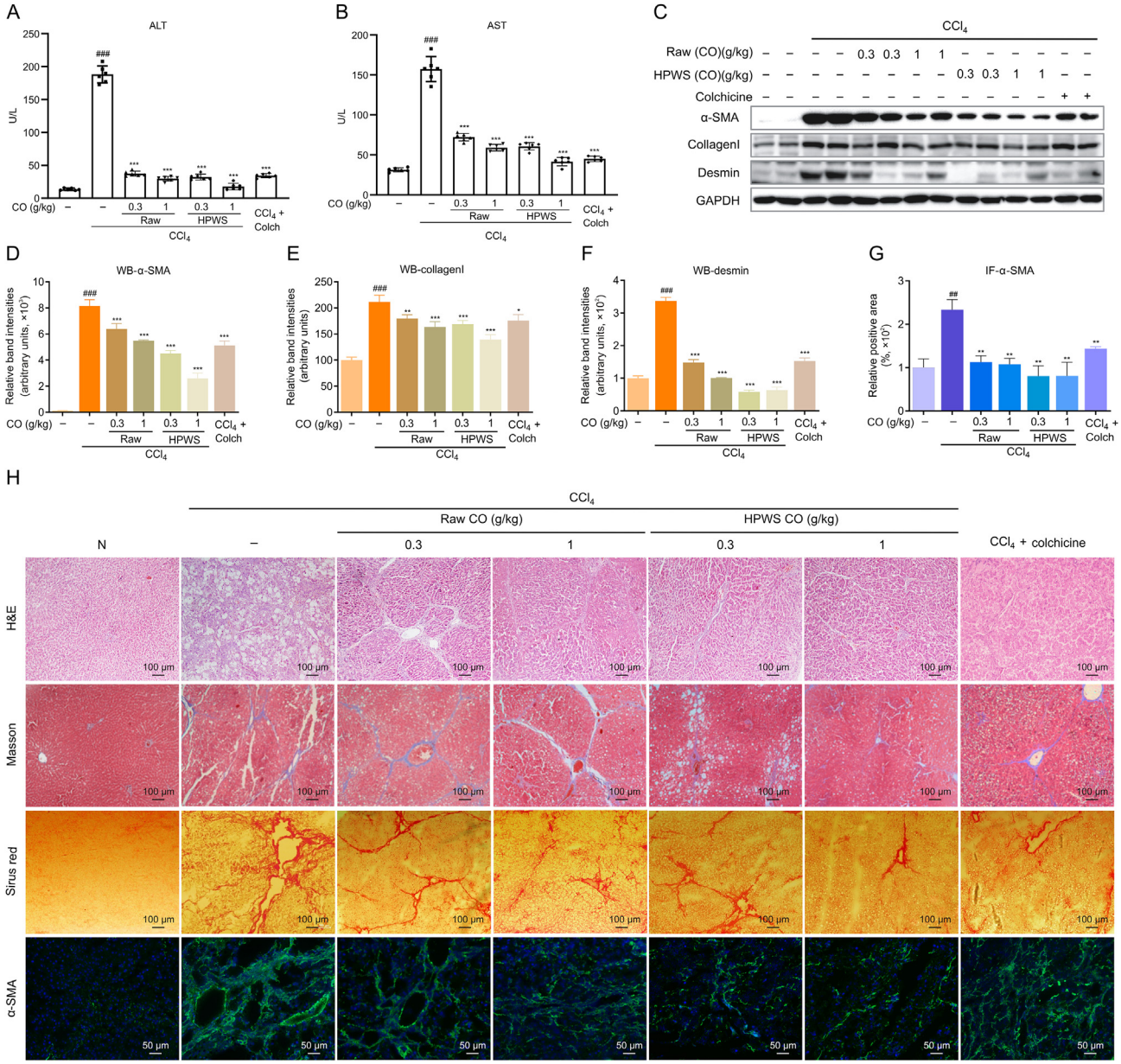

Fig. 1. *Cornus officinalis* (CO) relieved hepatic injury and hepatic fibrosis in the CCl_4 model. (A) Alanine aminotransferase (ALT) level in serum. (B) Aspartate aminotransferase (AST) level in serum. (C) Representative western blotting analysis (WB) for expressions of α-smooth muscle actin (α-SMA), CollagenI, Desmin and glyceraldehyde-3-phosphate dehydrogenase (GAPDH). (D–F) Relative band intensities for the protein expressions of α-SMA, CollagenI and Desmin, respectively. Densitometric values were normalized against GAPDH. (G) Relative positive area for immunofluorescence (IF) staining of α-SMA. (H) Hematoxylin and Eosin (H&E), Masson, Sirius red staining (100× original magnification) and IF staining of α-SMA (200× magnification). $^{\#\#}P < 0.01$, $^{\#\#\#}P < 0.001$, significantly different when compared with normal group; $^{*}P < 0.05$, $^{**}P < 0.01$, $^{***}P < 0.001$, significantly different when compared with CCl_4 group. HPWS: high pressure wine steaming.

$P < 0.05$. OPLS-DA analysis was carried out by the software SIMCA-P 14.1.

3. Results

3.1. *Cornus officinalis* relieved CCl_4-induced liver injury and fibrosis in rats

Firstly, the effects of *cornus officinalis* on heart, spleen, lung, kidney were assay by HE, showing that *cornus officinalis* with raw and HPWS at 1 g/kg had no systematic toxicity on rats (Fig. S1). Subsequently, to preliminarily exploring the effects of *cornus officinalis* on liver injury induced by CCl_4, serum aminotransferases analysis in rats were conducted in the present study. The results showed that levels of serum alanine aminotransferase (ALT) and aspartate aminotransferase (AST) increased by CCl_4 were reduced by *cornus officinalis* (Figs. 1A and B). It also verified that CCl_4 ingestion results in alterations of pro-fibrogenic factors, including α-SMA, collagenI and desmin (Figs. 1C—F). The result showed that these pro-fibrogenic factors were remarkably increased in CCl_4 compared with those in the normal group, while the treatment of *cornus officinalis* with or without HPWS can reversed these in a dose-dependent manner (Figs. 1C—F). The same alternation happened in the results of immunofluorescence for α-SMA, showing that CCl_4 significantly up-regulated α-SMA, and the administration of *cornus officinalis* with or without HPWS obviously down-regulated these protein expression levels induced by CCl_4 (Figs. 1G and H).

Moreover, the effects of *cornus officinalis* on liver histopathology were evidenced by H&E, Masson and Sirius Red staining data (Fig. 1H). To be specific, H&E result showed that treatment with *cornus officinalis* effectively improved liver histopathology (Fig. 1H). Consistently, the results of Masson and Sirius Red indicated that tissue collagen deposition was remarkable weakened by *cornus officinalis*, whether with or without HPWS treatments, in

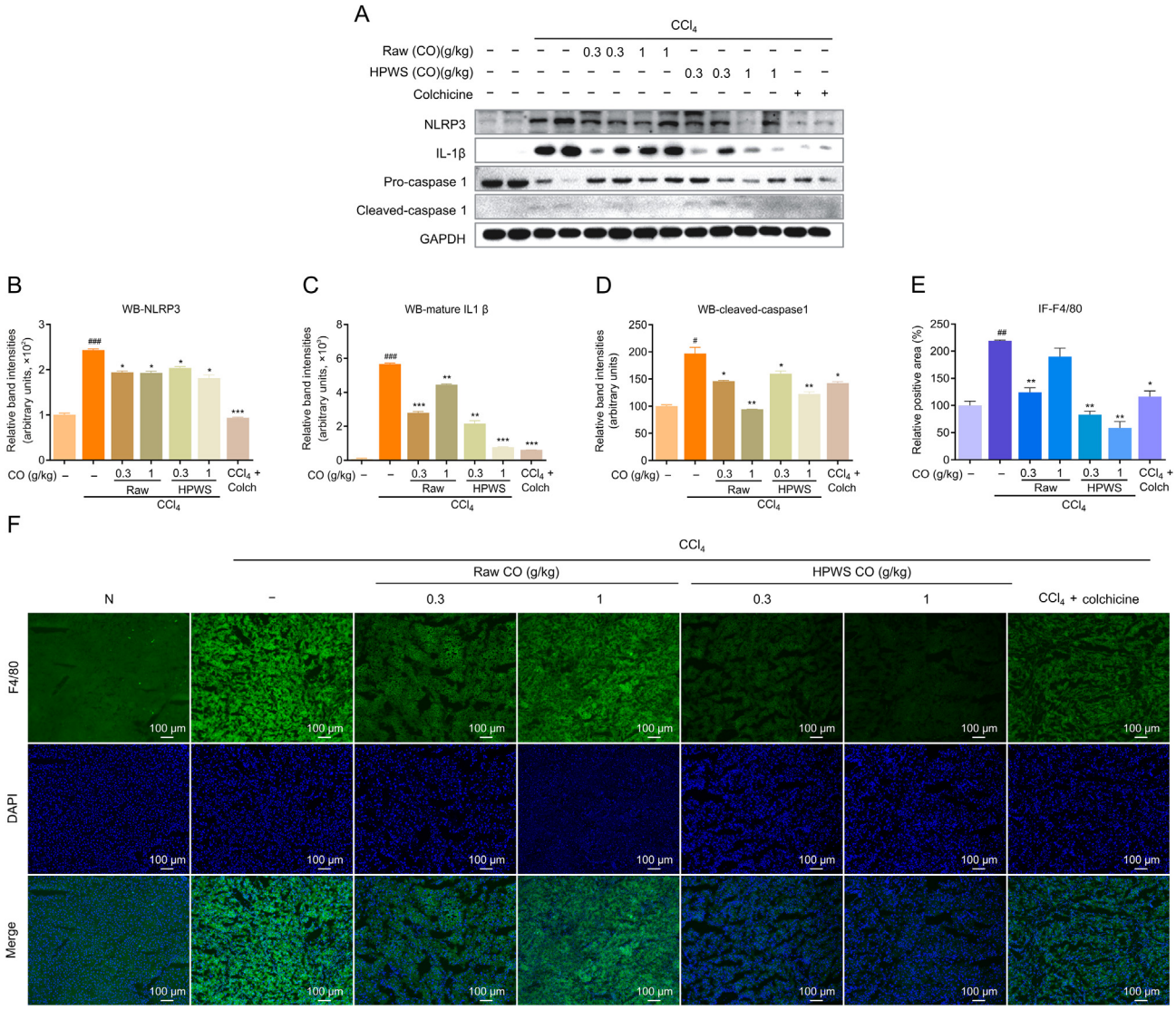

Fig. 2. *Cornus officinalis* (CO) attenuated the levels of pro-inflammatory cytokines. (A) Representative western blotting analysis (WB) for expressions of NOD-like receptor thermal protein domain associated protein 3 (NLRP3), interleukin (IL)-1β, caspase1 and glyceraldehyde-3-phosphate dehydrogenase (GAPDH). (B—D) Relative band intensities for the protein expressions of NLRP3, IL-1β and cleaved caspase1, respectively. Densitometric values were normalized against GAPDH. (E) Relative positive area for immunofluorescence (IF) staining of F4/80. (F) IF staining of F4/80 (100× magnification). $^{\#}P < 0.05$, $^{\#\#}P < 0.01$, $^{\#\#\#}P < 0.001$, significantly different when compared with normal group; $^{*}P < 0.05$, $^{**}P < 0.01$, $^{***}P < 0.001$, significantly different when compared with CCl_4 group. HPWS: high pressure wine steaming.

comparison to the CCl_4-exposed group (Fig. 1H). These findings manifested that CCl_4-exposure induced significant liver injury along with collagen deposition in CCl_4-injected rats, and this damage was ameliorated by the *cornus officinalis* administration. Importantly, the above results showed that the inhibitory effect of *cornus officinalis* with HPWS on liver injury and pro-fibrogenic factors was better than that of the raw form product.

3.2. *Cornus officinalis alleviates hepatic inflammation response*

Chronic or recurrent inflammation is closely related to persistent liver fibrosis. The onset of inflammation is often accompanied by the maturation of macrophage. Macrophage activation is manifested by the release of mature IL-1β, a process driven by the activation of NLRP3 and the subsequent increase in the cleavage of caspase1, a response notably heightened by CCl_4 (Figs. 2A–D). Although both the raw and HPWS products of *cornus officinalis* showed a similar effect on the activation of NLRP3 and the cleavage of caspase1, the impact of *cornus officinalis* with HPWS in inhibiting the release of IL-1β was significantly superior to that of the raw product (Figs. 2A–D). Moreover, F4/80, a mature macrophage marker, were also assessed by immunofluorescence staining. This analysis revealed that the injection of CCl_4 led to a significant increase in the expression of F4/80, which were reversed by *cornus officinalis* treatments (Figs. 2E and F). Therefore, *cornus officinalis* could relieve inflammation response, mainly manifest by inhibiting the release of inflammatory factors, and effect of *cornus officinalis* with HPWS was better than that of the raw form product.

3.3. *Identification of the compounds in cornus officinalis and its potential mechanism*

Pharmacodynamic differences are often closely related to changes in composition. To identify the compounds in *cornus officinalis*, UHPLC-QTOF-MS in combination with a literature search, MCnebula [32] established by our group were adopted to analysis the components contained in *cornus officinalis*, showing that the composition of the preparations was iridoid o-glycosides, iridoid and derivatives, flavonoid o-glycosides and others (Fig. S2). Subsequently, typical base peak and total ion chromatograms (TIC) are shown in Fig. 3A (raw) and Fig. 3B (HPWS). Fold change analysis was conducted by using the MetaboAnalyst website (https://www.metaboanalyst.ca/), revealing the general variation in the chemical composition of *cornus officinalis* in its raw and HPWS forms (Fig. 3C). Through a comparison of mass spectrometry date, mass spectrometry and fragmentation information, 41 major compounds were preliminarily identified in *cornus officinalis*. The detailed characteristics of each compound are shown in Table 1. Using a VIP value >1.0 as the filtering standard, 29 components in *cornus officinalis* had significant changes before and after HPWS. To discuss phytochemical and pharmacological relationship, take MO, an iridoid glycoside with anti-fibrosis effect, as an example. In the process of processing, MO broke the glucoside bond and dehydrated to form sarracenin (SA) (Fig. S3A). Moreover, activated HSCs were used to evaluate the anti-fibrosis effect of MO and SA, showing that the antifibrotic effect of SA was better than that of MO *in vitro* (Figs. S3B–D), which revealed connotation of processing effect enhancement of *cornus officinalis* to a certain extent.

To explore the mechanism behind the enhanced anti-hepatic fibrosis effects of *cornus officinalis* with HPWS, the database mentioned in the method were employed to screen potential targets for these 29 differential compounds. The analysis predicted a total of 805 targets, which are provided in Table S1. Furthermore, therapeutic targets for liver fibrosis were collected from various database, including Genecards, OMIM, and DisGeNET. After removing duplicates, we obtained 1844 disease targets, which are provided in Table S2. A Venn diagram was used to analyze the overlap between the predicted compound targets and therapeutic targets in liver fibrosis, potential targets for the treatment of liver fibrosis by *cornus officinalis* with HPWS (Fig. 3D). Additionally, KEGG enrichment analysis showed that these potential targets of *cornus officinalis* in the treatment of liver fibrosis were primarily

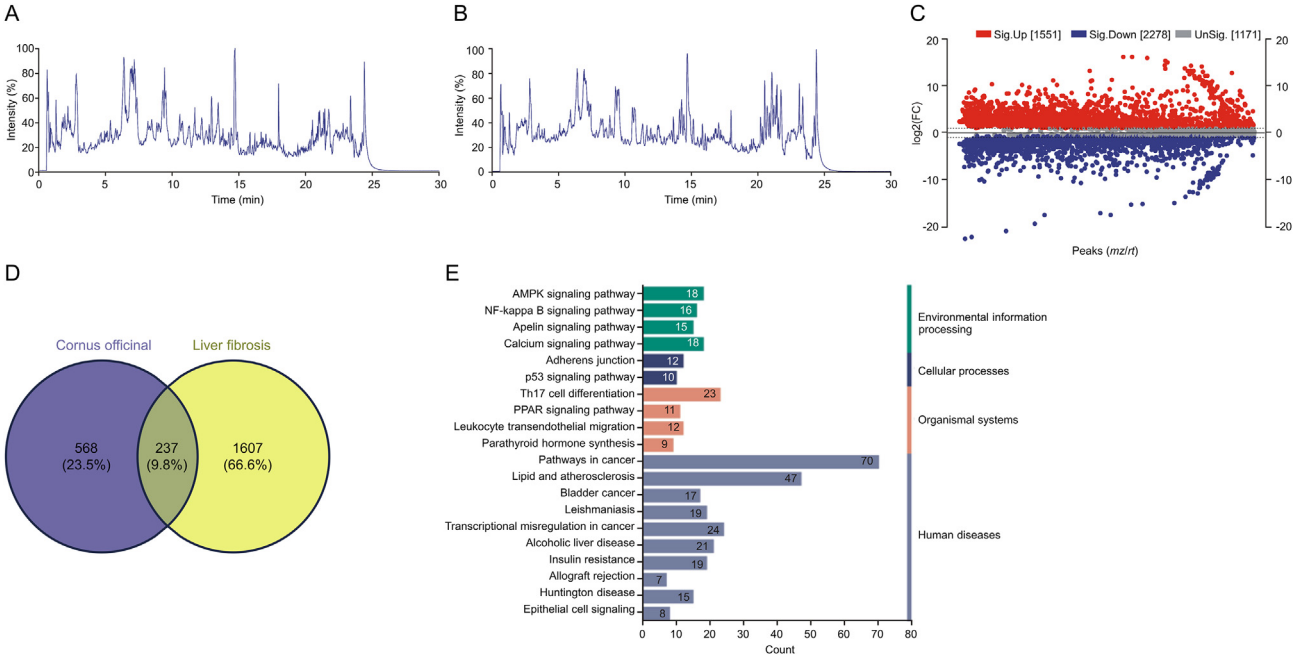

Fig. 3. Identification of the compounds in *cornus officinalis* and its potential mechanism. (A) Total ion chromatograms (TIC) chromatogram of raw *cornus officinalis* in negative mode. (B) TIC chromatogram of high pressure wine steaming (HPWS) *cornus officinalis* in negative mode. (C) The fold change plots of raw and HPWS *cornus officinalis*. (D) Venn diagram of 237 common target of *cornus officinalis* and liver fibrosis. (E) The top 20 significantly enriched terms in Kyoto Encyclopedia of Genes and Genomes (KEGG) pathways. AMPK: Adenosine 5'-monophosphate (AMP)-activated protein kinase; PPAR: peroxisome proliferators-activated receptor.

Table 1
Characterization of differential compounds of RAW and high pressure wine steaming (HPWS) *Cornus officinal* by UPLC-HRMS.

No.	RT (min)	Formula	Theoretical mass (Da)	Ion type	Actual mass (Da)	Error (ppm)	Identification	MS/MS ions (*m/z*)	Intensity trend
1	0.86	$C_4H_6O_6$	149.0086	$[M-H]^-$	149.0087	0.57	Tartaric acid	149.0092, 105.0209, 103.0012, 87.0089, 75.0084, 72.9923, 59.0136	↑
2	1.15	$C_4H_6O_5$	133.0137	$[M-H]^-$	133.0139	1.50	Malic acid	133.0140, 115.0034, 89.0233, 87.0075, 72.9926, 71.0138, 59.7812	↓
3	1.45	$C_6H_8O_7$	191.0192	$[M-H]^-$	191.0191	−0.42	Citric acid	191.0178, 129.0202, 87.0087, 85.0297, 57.4859	↓
4	2.07	$C_{14}H_{18}O_{11}$	361.0771	$[M-H]^-$	361.0776	1.41	7-O-Galloyl-D-sedoheptulose	361.0774, 271.0457, 241.0354, 211.0241, 183.0273, 169.0131, 125.0239	↓
5	2.22	$C_{13}H_{16}O_{10}$	331.0665	$[M-H]^-$	331.0672	2.04	3-O-Galloyl-D-glucose	331.0665, 271.0452, 241.0350, 211.0239, 183.0237, 169.0138, 167.0336, 151.0030, 125.0234, 123.0083, 119.0341, 113.0241, 107.0129, 101.0247, 89.0253, 71.0150, 59.0123	↓
6	2.53	$C_{13}H_{18}O_8$	337.1135	$[M+2H_2O-H]^-$	337.1134	−0.22	Tachioside	337.1145, 225.0595, 179.0563, 161.0466,149.0077, 143.0343,119.0340, 102.0231, 101.0253, 95.0213, 89.0230, 71.0157	↓
7	2.56	$C_7H_6O_5$	169.0137	$[M-H]^-$	169.0136	−0.59	Gallic acid	169.0136, 125.0240, 123.0077, 107.0137, 97.0294, 69.0350	↑
8	4.26	$C_7H_6O_4$	153.0188	$[M-H]^-$	153.0187	−0.56	Protocatechuic acid	153.0186, 109.0290	↑
9	5.38	$C_{13}H_{12}O_9$	311.0403	$[M-H]^-$	311.0408	1.58	Caftaric acid	311.0383, 223.0622, 179.0345, 149.0083, 135.0446	↓
10	5.91	$C_{23}H_{36}O_{16}$	613.1980	$[M+COOH]^-$	613.1978	−0.32	Eriobioside	613.1972, 567.1916, 507.1640, 477.1740, 405.1385, 345.1143, 315.1075, 297.0963, 285.0977, 243.0867, 225.0762, 179.0537, 161.0442, 143.0337, 113.0237, 101.0240, 89.0221	↑
11	6.46	$C_{16}H_{24}O_{10}$	375.1291	$[M-H]^-$	375.1293	0.47	Loganic acid	375.1294, 213.0763, 169.0862, 151.0761, 119.0341, 101.0237, 99.0446, 95.0492, 89.0241, 71.0125, 69.0353, 59.0153	↓
12	7.04	$C_{17}H_{26}O_{11}$	451.1452	$[M+COOH]^-$	451.1457	1.17	Morroniside	451.1465, 405.1406, 243.0874, 179.0554, 161.0458, 119.0342, 113.0239, 101.0240, 89.0247, 59.0141	↓
13	7.42	$C_{16}H_{22}O_{11}$	389.1084	$[M-H]^-$	389.1092	2.08	Secologanoside	389.1092, 345.1183, 209.0452, 183.0663, 179.0542, 165.0551, 149.0470,139.0024, 121.0650, 119.0359, 113.0242, 101.0240, 89.0221, 85.0322, 71.0141, 69.0337, 59.0151	↓
14	7.89	$C_6H_{12}O_6$	179.0556	$[M-H]^-$	179.0573	9.69	Fructose	179.0343, 119.0429, 89.0472, 85.0917, 71.4407, 59.3661	↑
15	7.89	$C_9H_8O_4$	179.0344	$[M-H]^-$	179.0343	−0.75	Caffeic acid	179.0343, 135.0444, 117.0383, 107.0499	↑
16	8.35	$C_{41}H_{30}O_{27}$	953.0896	$[M-H]^-$	953.0903	0.70	Rugosin B	953.0953, 909.0967, 783.0697, 483.0725, 300.9990, 176.9127	↑
17	8.44	$C_{18}H_{24}O_{12}$	431.1190	$[M-H]^-$	431.1204	3.35	Asperulosidic acid	431.0987, 251.0453, 165.0110, 146.9762, 119.0114	↓
18	8.52	$C_{34}H_{26}O_{22}$	785.0838	$[M-H]^-$	785.0837	−0.07	Tellimagrandin I	785.0830, 633.0693, 615.0641, 483.0765, 419.0615, 300.9988, 275.0193, 249.0398, 169.0136	↓
19	9.28	$C_{17}H_{24}O_{10}$	433.1346	$[M+COOH]^-$	433.1349	0.68	Verbenalin	433.1356, 225.0766, 125.0255, 101.0239	↑
20	9.29	$C_{16}H_{22}O_{10}$	433.1346	$[M+CH_3COO]^-$	433.1349	0.68	Swertiamarin	433.1356, 225.0766, 123.0435, 101.0239	↑
21	9.35	$C_{16}H_{22}O_9$	403.1240	$[M+COOH]^-$	403.1246	1.39	Sweroside	403.1245, 357.1178, 195.0653, 179.0530, 177.0557, 151.0757, 125.0241, 119.0330, 89.0255, 59.0157	↓
22	9.36	$C_{15}H_{16}O_9$	339.0716	$[M-H]^-$	339.0722	1.74	Cafeoyltartaric acid dimethyl ester	339.0823, 179.0345, 177.0393, 161.0231, 159.0300, 135.0444, 133.0252, 129.0173	↑
23	9.46	$C_{17}H_{26}O_{10}$	435.1503	$[M+COOH]^-$	435.1515	2.86	Loganin	435.1519, 389.1425, 227.0922, 101.0241	↓
24	9.84	$C_{23}H_{34}O_{15}$	609.2031	$[M+CH_3COO]^-$	609.204	1.51	7-β-O-dimethyl butanedioate morroniside	609.2034, 389.1468, 227.0923, 173.0451, 127.0387, 101.0262	↑
25	10.46	$C_9H_8O_3$	163.0395	$[M-H]^-$	163.0394	−0.74	P-hydroxycinnamic acid	163.0395, 119.0494, 117.0381, 104.0227, 93.0343, 91.0559	↑
26	10.61	$C_{21}H_{30}O_{14}$	505.1557	$[M-H]^-$	505.1554	−0.66	Cornuside III	505.1560, 227.0919, 127.0396, 115.0038, 101.0237, 71.0138	↑
27	11.38	$C_{21}H_{30}O_{14}$	505.1557	$[M-H]^-$	505.157	2.50	Cornuside IV	505.1562, 227.0924, 127.0409, 115.0033, 101.0236, 71.0135	↑
28	12.22	$C_{34}H_{28}O_{22}$	787.0994	$[M-H]^-$	787.0993	−0.13	1,2,3,6-Tetra-O-galloyl-β-D-glucose	787.0978, 635.0881, 617.0770, 483.0717, 447.0560, 313.0553, 169.0132, 125.0226	↓
29	12.56	$C_{14}H_6O_8$	300.9984	$[M-H]^-$	300.9994	3.17	Ellagic acid	300.9992, 257.0084, 245.0094	↑
30	12.92	$C_{18}H_{28}O_{11}$	419.1553	$[M-H]^-$	419.1516	−8.92			↑

(*continued on next page*)

Table 1 (*continued*)

No.	RT (min)	Formula	Theoretical mass (Da)	Ion type	Actual mass (Da)	Error (ppm)	Identification	MS/MS ions (*m/z*)	Intensity trend
31	12.99	$C_{21}H_{18}O_{13}$	477.0669	$[M-H]^-$	477.0678	1.84	7-O-Methylmorroniside	419.0943, 373.1246, 211.0600, 181.0595, 101.0156, 71.0007	→
32	12.99	$C_{19}H_{30}O_{11}$	433.1710	$[M-H]^-$	433.1716	1.41	Querciturone	477.0681, 301.0359, 151.0033	←
33	14.66	$C_{24}H_{30}O_{14}$	541.1557	$[M-H]^-$	541.1565	1.41	7-O-Ethyl-morroniside	433.1801, 397.1307, 271.0478, 253.1524	←
34	16.25	$C_{15}H_{12}O_7$	303.0505	$[M-H]^-$	303.0508	1.06	Cornuside I	541.1572, 347.0771, 309.0613, 169.0149, 125.0239	←
35	17.07	$C_{15}H_{10}O_7$	301.0348	$[M-H]^-$	301.035	0.56	Dihydroquercetin	303.0506, 183.0293, 165.0185, 139.0397, 137.0241, 93.0328	←
36	17.99	$C_{36}H_{58}O_{10}$	695.4007	$[M+COOH]^-$	695.3983	−3.39	Quercetin	301.0346, 271.0239, 255.0233, 245.0071, 227.1958, 151.0454	←
37	18.02	$C_{15}H_{10}O_6$	285.0399	$[M-H]^-$	285.0403	1.35	Arjunglucoside II	695.3990, 649.4009, 487.3422	→
38	21.73	$C_{30}H_{48}O_4$	471.3474	$[M-H]^-$	471.3476	0.35	Kaempferol	285.0401, 255.0289, 163.0006, 159.0474, 107.0075	←
39	21.91	$C_{30}H_{48}O_4$	471.3474	$[M-H]^-$	471.3465	−1.98	Maslinic acid	471.3474	→
40	23.39	$C_{30}H_{48}O_3$	455.3525	$[M-H]^-$	455.3537	2.59	Corosolic acid	471.3475	→
41	23.6	$C_{30}H_{48}O_3$	455.3525	$[M-H]^-$	455.3526	0.18	Oleanolic acid	455.3535	→
							Ursolic acid	455.35275	→

concentrated in the AMPK signaling pathway (Fig. 3E). These results suggested that the mechanism of enhanced anti-fibrosis effect of *cornus officinalis* processing may be related to AMPK pathway.

3.4. *Cornus officinalis* regulates SIRT3-AMPK way and attenuates apoptosis in CCl_4-induced rats

The fact that AMPK plays a critical role in inflammation and fibrosis and its protective role in liver has been extensive reported [33–35]. Moreover, SIRT3, a deacetylase that consist in mitochondrial membrane, can participate in the phosphorylation modification of AMPK [36]. To explore whether *cornus officinalis* can ameliorate liver fibrosis by regulating SIRT3-AMPK, molecular biological techniques, including western blotting analysis and immunofluorescence staining were employed in our present study (Fig. 4). The results showed that the protein expression of SIRT3 was significantly decreased in the CCl_4 group compared to the normal group, whereas treatment with *cornus officinalis*, both its raw and HPWS form, as well as colchicine, significantly elevated the SIRT3 expression (Figs. 4A and B). Consistently, immunofluorescence results showed that CCl_4 treatment reduced the positive expression area (in green) of SIRT3, which was significantly enhanced by *cornus officinalis* in both raw and HPWS or colchicine (Figs. 4C and E). Moreover, immunofluorescence staining was employed to investigate whether the regulatory effect of *cornus officinalis* on AMPK is related to SIRT3, showing that the phosphorylation expressions of AMPK were significantly decreased in CCl_4 group compared with the normal, while the treatment of *cornus officinalis* in both raw and HPWS products or colchicine could reverse these. Notably, the regulation of *cornus officinalis* HPWS treatment on AMPK a was better than its raw product and positive control (Figs. 4D and E). We can see that the improvement of *cornus officinalis* on liver fibrosis induced by CCl_4 is associated with the expression of SIRT3 and AMPK.

To illustrate the suppression of CCl_4-induced liver apoptosis by *cornus officinalis*, we detected the levels of several factors related to apoptotic pathways, including the caspase family and the Bcl-2 family. The results showed that CCl_4 injection significantly increased the levels of cleaved caspase-3, caspase-6 and caspase-9, all of which were decreased by *cornus officinalis* treatments (Figs. 4F–I). Moreover, the expression of Beclin 1 was notably increased, and Bcl2 was significantly reduced in the CCl_4 group when compared with the normal group, however, the administration of *cornus officinalis* could reverse these compared with the CCl_4 group (Figs. 4F, J and K), among which, *cornus officinalis* with HPWS showed better effects than its raw product. These findings were further confirmed by immunofluorescence results for caspase-6, which showed that the positive area (in green) of caspase-6 in the CCl_4 group was greater than in the normal group but less than in the groups treated with *cornus officinalis* with or without HPWS administrations as well as colchicine administrations (Figs. 4L and M). The above results showed that the anti-fibrosis effect of *cornus officinalis* is connected with the attenuation of apoptosis in liver, which may be related to the SIRT3-AMPK pathway.

3.5. *Cornus officinalis* inhibits the expression of pro-fibrotic factors in HSC-T6

To evaluate the antifibrotic activity of *cornus officinalis* at safe dose *in vitro*, the MTT assay was applied to evaluate its cytotoxicity on HSC-T6 cells in both quiescent and activated state. The results indicated that *cornus officinalis* at doses ranging from 0 to 250 μg/mL showed minimal cytotoxicity (Figs. 5A and B). Taking this into account, doses of 50 and 250 μg/mL were selected for use in subsequent experiments. *In vitro*, the protein expressions of fibrosis

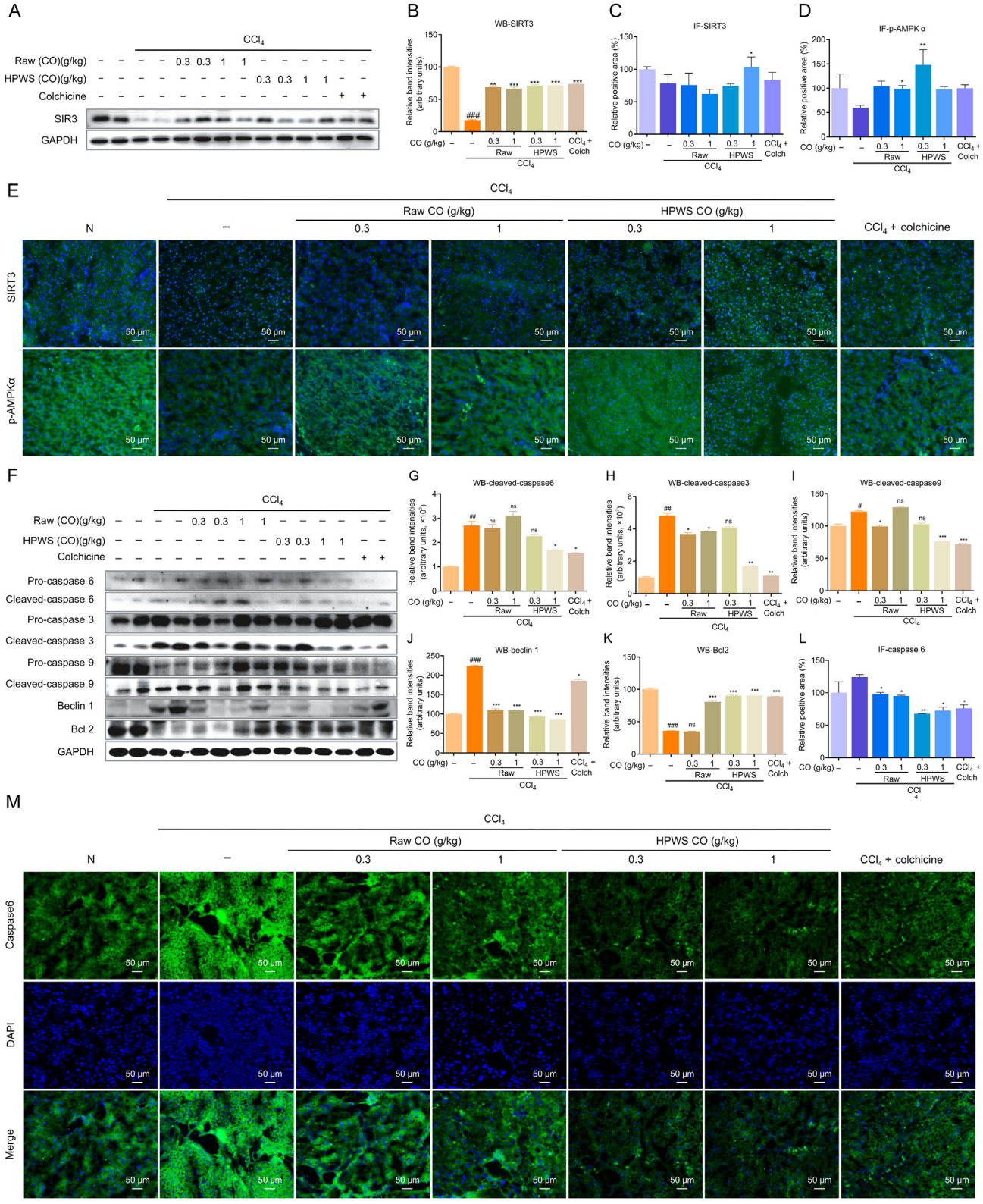

Fig. 4. *Cornus officinalis* (CO) regulates Sirtuin 3 (SIRT3)-adenosine 5'-monophosphate (AMP)-activated protein kinase way and inhibits hepatic apoptosis in CCl_4 induced mice. (A) Representative western blotting analysis (WB) for expressions of SIRT3 and glyceraldehyde-3-phosphate dehydrogenase (GAPDH). (B) Relative band intensities for the protein expression of SIRT3. Densitometric values were normalized against GAPDH. (C and D) Relative positive areas for immunofluorescence (IF) staining of SIRT3 and (AMP)-activated protein kinase, AMPK (p-AMPK) α, respectively. (E) IF staining of p-AMPKα and SIRT3 (200× magnification). (F) Representative western blotting analysis for expressions of caspase3, caspase6, caspase9, Beclin1, Bcl2 and GAPDH. (G–K) Relative band intensities for the protein expressions of cleaved caspase3, cleaved caspase6, cleaved caspase9, Beclin1 and B-cell lymphoma-2 (Bcl2), respectively. Densitometric values were normalized against GAPDH. (L) Relative positive areas for IF staining of caspase6. (M) IF staining of caspase 6 (200× magnification). $^{\#}P < 0.05$, $^{\#\#}P < 0.05$, $^{\#\#}P < 0.001$, significantly different when compared with normal group; $^{*}P < 0.05$, $^{**}P < 0.01$, $^{***}P < 0.001$, significantly different when compared with CCl_4 group, ns.: no statistical significance; HPWS: high pressure wine steaming.

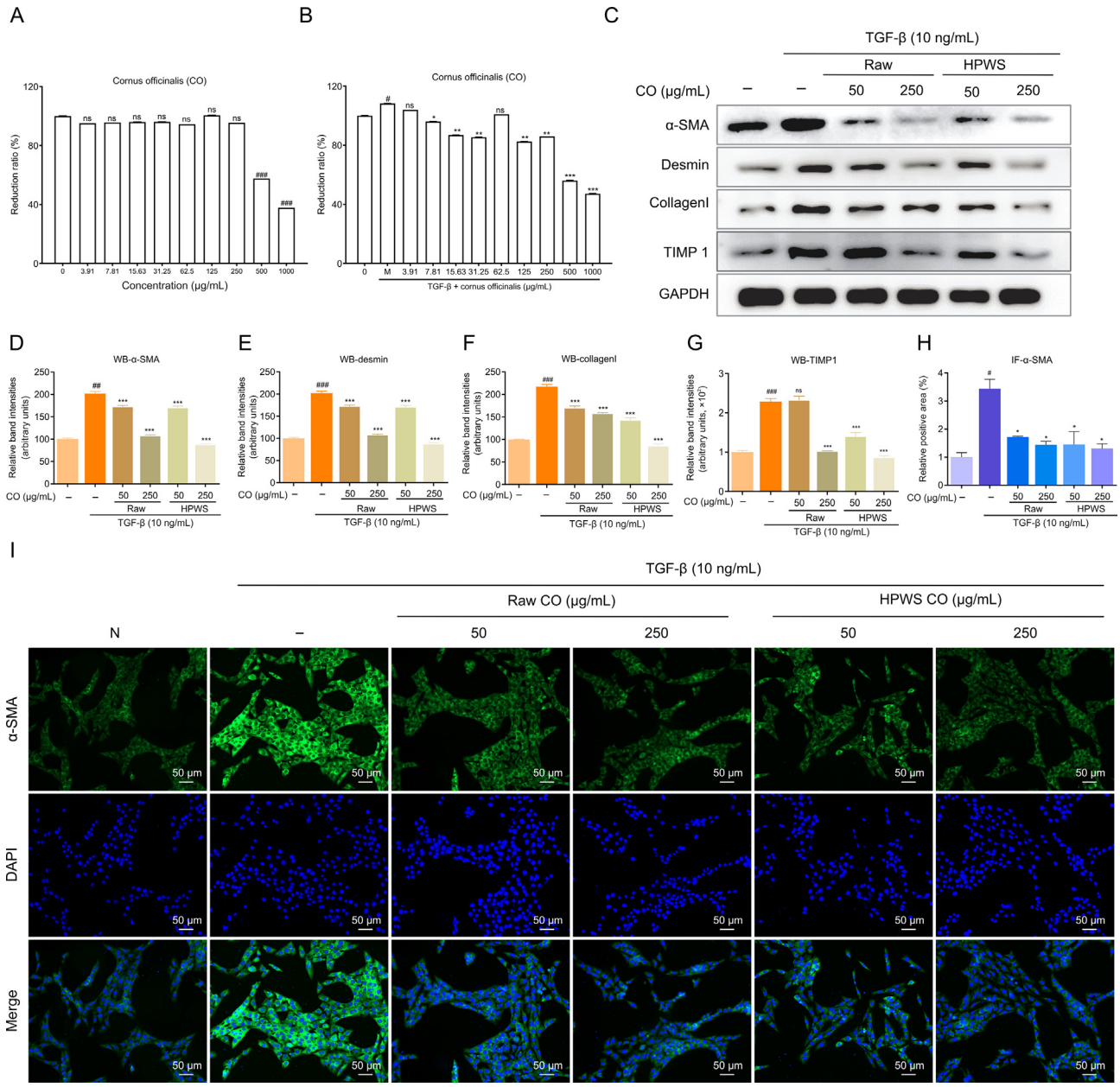

Fig. 5. *Cornus officinalis* (CO) inhibited hepatic fibrosis markers in transforming growth factor-β (TGF-β)-activated HSC-T6. (A) Cell viability of HSC-T6 treated with CO. (B) Cell viability of TGF-β stimulated HSC-T6 treated with *cornus officinalis*. (C) Representative western blotting analysis for expressions of α-smooth muscle actin (α-SMA), desmin, collagenI, Tissue Inhibitors of Metalloproteinase 1 (TIMP1) and glyceraldehyde-3-phosphate dehydrogenase (GAPDH). (D–G) Relative band intensities for the protein expressions of α-SMA, desmin, collagenI and TIMP1, respectively. Densitometric values were normalized against GAPDH. (H) Relative positive areas for IF staining of α-SMA. (I) IF staining of α-SMA (200× magnification). $^{\#}P < 0.05$, $^{\#\#}P < 0.01$, $^{\#\#\#}P < 0.001$, significantly different when compared with normal group; $^{*}P < 0.05$, $^{**}P < 0.01$, $^{***}P < 0.001$, significantly different when compared with TGF-β group, ns: no statistical significance; HPWS: high pressure wine steaming.

index were significantly increased in HSC-T6 cells activated by TGF-β, such as α-SMA, collagenI, desmin and TIMP1, which means the production and deposition of ECM proteins, while *cornus officinalis* both in raw and HPWS forms could suppress these increases induced by TGF-β (Figs. 5C–G). To further verify the *in vitro* anti-fibrotic effect of *cornus officinalis*, immunofluorescence staining was applied in current study. It demonstrated that the augmented positive expression (in green) of α-SMA was significantly reduced by *cornus officinalis* both in raw and HPWS treatment (Figs. 5H and I), with the therapeutic effects of *cornus officinalis* in HPWS form better. It was confirmed that the anti-fibrosis activity of *cornus officinalis* was related to the inhibition of HSCs activation.

3.6. *Cornus officinalis promotes apoptosis and regulates expression of SIRT3-AMPK axis in TGFβ-induced HSC-T6 cells*

In contrast to ameliorate hepatocytes apoptosis *in vivo*, promoting the apoptosis of activated HSCs is a promising strategy for the therapy of liver fibrosis [37]. Next, the effect of *cornus officinalis* on expressions of factors that related to apoptotic pathways in activated HSC-T6 was examined in the present study, showing the levels of cleaved caspase-3, caspase-6 and caspase-9 were enhanced by *cornus officinalis* both in raw and HPWS treatment (Figs. 6A–D). Similarly, the results of flow cytometry experiments showed that the cell apoptosis in *cornus officinalis* group (especially

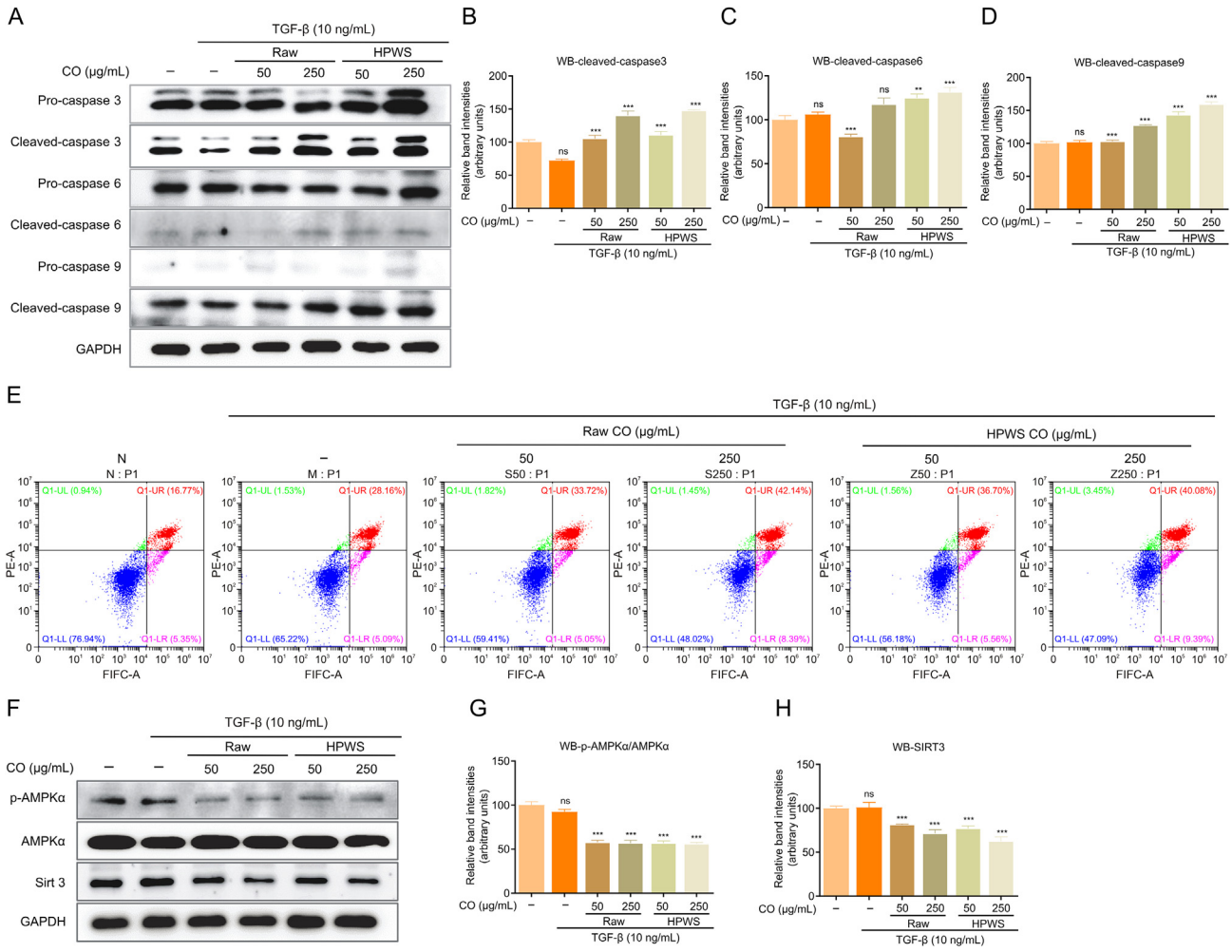

Fig. 6. *Cornus officinalis* (CO) promotes apoptosis and regulates expression of sirtuin (SIRT3)-adenosine monophosphate-activated protein kinase (AMPK) axis in transforming growth factor (TGF) β-induced HSC-T6 cells. (A) Representative western blotting analysis (WB) for expressions of caspase3, caspase6, caspase9 and GAPDH. (B–D) Relative band intensities for the protein expressions of cleaved caspase3, cleaved caspase6 and cleaved caspase9, respectively. Densitometric values were normalized against glyceraldehyde-3-phosphate dehydrogenase (GAPDH). (E) Flow cytometry assay of apoptosis induction in treated HSC-T6 cells. (F) Representative WB for expressions of SIRT3, AMPK*α*, p-AMPK*α* and GAPDH. (G and H) Relative band intensities for the ratio of p-AMPK*α*/AMPK*α* and SIRT3, respectively. Densitometric values were normalized against GAPDH. $^{**}P < 0.01$, $^{***}P < 0.001$, significantly different when compared with TGF-β group. ns: no statistical significance; HPWS: high pressure wine steaming.

with HPWS) was more than those in TGF-β group (Fig. 6E), all of which indicated that *cornus officinalis* could improve liver fibrosis via induction of HSC-T6 apoptosis.

As what has been mentioned above, the activation of SIRT3 and AMPK is related to the protection of *cornus officinalis* against hepatocytes apoptosis *in vivo*. In order to explore whether the pro-apoptotic effect of *cornus officinalis* on HSC-T6 is also associated with the expressions of SIRT3 and AMPK, western blotting was used to detect these indicators in activated HSC-T6. The results showed that the expression of SIRT3 was decreased by *cornus officinalis* in a dose-dependent manner compared with TGF-β group, along with decrease AMPK phosphorylation (Figs. 6F–H). This result also suggested that regulation of the SIRT3-AMPK axis represents a potential therapeutic target of *cornus officinalis* against liver fibrosis.

3.7. *Cornus officinalis promotes AMPK-mediated apoptosis through SIRT3 in TGFβ-induced HSC-T6 cells*

The present study preliminarily evaluated that *cornus officinalis* can play an anti-fibrosis role by promoting activated HSCs apoptosis, which is related to SIRT3-AMPK axis *in vivo* and *in vitro* experiments. To clarify this mechanism, lentivirus was used to construct SIRT3-knockdown HSC-T6 cells (Figs. 7A–C). Compared to control RNAi, the reduction of SIRT3 leading to a decrease in the phosphorylation level of AMPK, indicated the inactivation of AMPK (Figs. 7D–G). Moreover, the decrease of SIRT3 also affected the regulation of AMPK by *cornus officinalis*, which can be seen from the results of western blotting and immunofluorescence staining, specifically, the phosphorylation of AMPK in SIRT3 RNAi group treatment with *cornus officinalis* was significantly reduced compared to that in control RNAi group, among which *cornus officinalis* with HPWS had the strongest regulatory effect (Figs. 7D–G). It can be concluded that *cornus officinalis* can regulate AMPK activity through SIRT3.

Once phosphorylation of AMPK was decreased, caspase-6 was activated by caspase-3 along with apoptotic reaction [23]. Next, whether the pro-apoptotic effect of *cornus officinalis* on HSC-T6 was related to the expression of SIRT3 was specifically investigated in the present study. The results showed that compared with the control RANi, SIRT3 knockdown and *cornus officinalis* treatment could lead to increases on cleavage of caspase3, caspase6 and

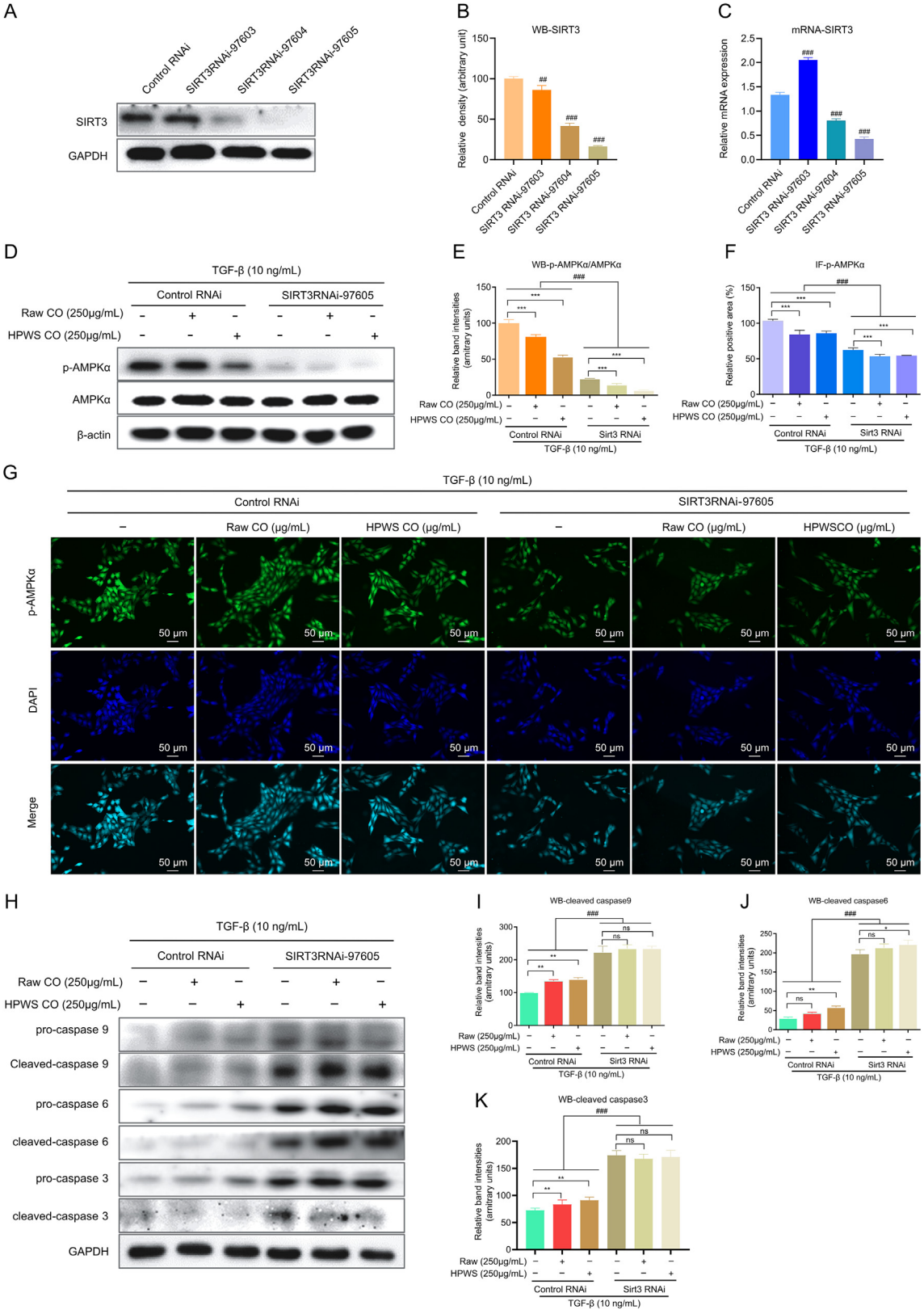

Fig. 7. *Cornus officinalis* (CO) promotes adenosine monophosphate-activated protein kinase (AMPK)-mediated apoptosis through SIrtuin 3 (SIRT3) in transforming growth factor (TGF)β-induced HSC-T6 cells. (A) Representative western blotting analysis (WB) for expressions of SIRT3 and glyceraldehyde-3-phosphate dehydrogenase (GAPDH). (B) Relative band intensities for the protein expressions of SIRT3. Densitometric values were normalized against GAPDH. (C) Relative mRNA expression of SIRT3. (D) Representative WB for expressions of AMPKα, p-AMPKα and β-actin. (E) Relative band intensities for the ratio of p-AMPKα/AMPKα. (F) Relative positive areas for IF staining of p-AMPKα. (G) IF staining of p-AMPKα (200× magnification). (H) Representative western blotting analysis for expressions of caspase9, caspase6 and caspase3. (I–K) Relative band intensities for the expressions of cleaved caspase9, cleaved caspase6 and cleaved caspase3. Densitometric values were normalized against GAPDH. $^{\#\#}P < 0.01$, $^{\#\#\#}P < 0.001$, significantly different when compared with control RNAi group; $^{*}P < 0.05$, $^{**}P < 0.01$, $^{***}P < 0.001$, significantly different when compared with TGF-β alone plus control RNAi or Sirt3 RANi treatment group. ns: no statistical significance; HPWS: high pressure wine steaming.

caspase9, while compared with the SIRT3 knockdown group, *cornus officinalis* treatment has no little significant regulatory effect on the above apoptosis-related factors, suggesting that *cornus officinalis* can regulate AMPK and mediated apoptosis through SIRT3 (Figs. 7H−K). Due to these results, it revealed that *cornus officinalis* can regulate AMPK and mediated apoptosis through SIRT3.

4. Discussion

Liver fibrosis is the consequence of chronic liver disease induced by different etiologies, and represents an inevitable stage in the progression to liver cirrhosis and, in severe cases, even cancer. Therefore, therapies targeting liver injury, inflammation, and fibrosis hold potential as treatment to prevent the development of cirrhosis in hepatic disease. However, there are currently very few medications approved by the FDA for this purpose. Given these considerations, the present study has focused on exploring candidate treatment for liver fibrosis with low side effects and well-defined mechanism. Recently, attention has shifted towards edible and herbal plants, such as *cornus officinalis*, which have gained substantial attention as nutritional products due to their potential to support liver and kidney health [8]. This study has indicated that *cornus officinalis* alleviated liver fibrosis induced by CCl_4 injection, particularly in its HPWS form. This effect is primarily achieved through modulating SIRT3-AMPK, where *cornus officinalis* inhibits liver inflammation, reduces apoptosis, and promotes the apoptosis of HSCs.

To elucidate the anti-fibrosis effect of both raw and HPWS *cornus officinalis*, CCl_4-induced liver fibrosis models and TGFβ-induced HSC-T6 activation were established. The results showed that CCl_4 injection led to the increase in the levels of serum ALT and AST, all of which were weakened by *cornus officinalis* administration, especially the HPWS form. *Cornus officinalis* significantly decreased fibrosis-related markers both *in vivo* and *vitro* settings, indicating the anti-fibrotic potential. Moreover, the activation of the NLRP3 inflammasome is known to play an important role in the initiation of the inflammatory response, a crucial stage in the development of liver fibrosis [8]. The current research also verified that upregulation of NLRP3 expression by CCl_4 was synchronized with its downstream cytokines, such as caspase1 and IL-1β. During these processes, NLRP3 can bind with ASC and caspse1, leading to the cleavage of caspase1 into its active form, cleaved caspase1, all of which in turn stimulates the cleavage of pro-IL-1β into its mature form [38]. Importantly, *cornus officinalis*, especially its HPWS form, could reverse the expressions of NLRP3, cleaved caspase1, and IL-1β in the liver fibrosis model. This finding indicated that *cornus officinalis*, especially when prepared as HPWS can enhance its anti-hepatic fibrosis properties.

The effect of *cornus officinalis* with HPWS on inflammation and fibrosis better than its raw form was related to composition that changed between the two. To identify these differential compounds, UHPLC-QTOF-MS combined with multivariate statistical analysis was employed. Based on these differential compounds, network analysis highlighted the AMPK signaling pathway as a potential mechanism. Consistently, the phosphorylation level of AMPK was significantly reduced in CCl_4-induced liver fibrosis. Subsequently, cells underwent apoptosis rapidly, along with expressions of apoptosis-related factor, including caspase 3, caspase 6, and caspase 9 [23], all of which were induced by CCl_4 and reversed by *cornus officinalis*, especially its HPWS form. Moreover, *cornus officinalis* can also regulate the expression of AMPK *in vitro* and accelerate the apoptosis of activated HSCs cells, thereby ameliorating liver fibrosis. Therefore, the main mechanism behind the anti-fibrotic enhancement of *cornus officinalis* with HPWS could be the AMPK mediated caspase pathway.

AMPK acts as a sensor of intracellular energy and its phosphorylation are often affected by changes in intracellular ATP levels [39]. SIRT3 deficiency results in increased levels of mitochondrial acetylation, effectively shifting mitochondrial function from ATP synthesis to reactive oxygen species production [40]. To clarify the relationship between the regulatory effect of *cornus officinalis* on AMPK and SIRT3, the expression of SIRT3 in CCl_4-induced liver fibrosis was assessed. We also constructed HSC-T6 cells with lentivirus-mediated SIRT3 RNAi, confirming the effect of *cornus officinalis* on AMPK activity through SIRT3. Moreover, the knockdown of SIRT3 affected the pro-apoptotic effect of *cornus officinalis* on activated HSC-T6. Overall, our studies reveal the anti-liver fibrosis effects of *cornus officinalis* in CCl_4-induced rats and TGF-β stimulated HSC-T6 cells are linked to the SIRT3-AMPK axis.

5. Conclusion

In this study, both *in vivo* and *in vitro* experiments have confirmed that *cornus officinalis* can relieve the progression of liver fibrosis via the SIRT3-AMPK axis. These findings offering valuable insights into the results may provide directions to better understand the underlying the mechanism of *cornus officinalis* with HPWS in the prevention of liver fibrosis, and they may open new avenues for *cornus officinalis* to be explored as a dietary food that can contribute to the prevention of liver fibrosis.

CRediT author statement

Xin Han: Investigation, Funding acquisition, Statistical analysis, Writing - Original draft preparation; **Yan Ning**: *In vivo* experiments, Statistical analysis, Network pharmacology, Methodology; **Xinyue Dou**: *In vitro* experiments, Methodology, Data curation; **Yiwen Wang**: Statistical analysis, Cell transfection; **Qiyuan Shan**: UHPLC-QTOF-MS, Language editing; **Kao Shi**: Animal feeding; **Zeping Wang**: Histological analysis; **Chuan Ding**: Cell culture; **Min Hao**: Statistical analysis; **Kuilong Wang**: Preparations of cornus officinalis; **Mengyun Peng**: Validation; **Haodan Kuang**: Funding acquisition; **Qiao Yang**: Validation; **Xianan Sang**: Writing - Reviewing and Editing, Supervision, **Gang Cao**: Writing - Reviewing and Editing, Supervision, Funding.

Declaration of competing interest

The authors declare that there are no conflicts of interest.

Acknowledgements

This work was financially supported by the National Natural Science Foundation of China (Grant Nos.: 82104394 and 81973481), the Natural Science Foundation of Zhejiang Province (Grant Nos.: Y23H280008 and LZ22H280001), Zhejiang Province Traditional Chinese Medicine Science and Technology Project (Grant No.: 2022ZQ033), Zhejiang Chinese Medicine University University-Level Talent Special Project (Grant No.: 2021ZR06), and Zhejiang Province Postdoctoral Research Project (Grant No.: ZJ2022057). Thanks to Professor Hongxia Zhang from Foreign Language Department, Zhejiang Chinese Medicine University for help in language editing. We appreciate the great help/technical support/experimental support from the Pharmaceutical Research Center, Academy of Chinese Medical Sciences, Zhejiang Chinese Medical University.

Appendix A. Supplementary data

Supplementary data to this article can be found online at https://doi.org/10.1016/j.jpha.2023.12.017.

References

[1] W. Fan, T. Liu, W. Chen, et al., ECM1 prevents activation of transforming growth factor β, hepatic stellate cells, and fibrogenesis in mice, Gastroenterology 157 (2019) 1352–1367.e13.
[2] X. Han, Y. Wu, Q. Yang, et al., Peroxisome proliferator-activated receptors in the pathogenesis and therapies of liver fibrosis, Pharmacol. Ther. 222 (2021), 107791.
[3] S.L. Friedman, M. Pinzani, Hepatic fibrosis 2022: Unmet needs and a blueprint for the future, Hepatology 75 (2022) 473–488.
[4] M. Chen, Y. Xie, S. Gong, et al., Traditional Chinese medicine in the treatment of nonalcoholic steatohepatitis, Pharmacol. Res. 172 (2021), 105849.
[5] X. Li, D. Zhou, X. Chi, et al., Entecavir combining Chinese herbal medicine for HBeAg-positive chronic hepatitis B patients: A randomized, controlled trial, Hepatol. Int. 14 (2020) 985–996.
[6] L. Zhang, G. Wang, W. Hou, et al., Contemporary clinical research of traditional Chinese medicines for chronic hepatitis B in China: An analytical review, Hepatology 51 (2010) 690–698.
[7] Y. Xing, W. Zhong, D. Peng, et al., Chinese herbal formula Ruangan Granule enhances the efficacy of entecavir to reverse advanced liver fibrosis/early cirrhosis in patients with chronic HBV infection: A multicenter, randomized clinical trial, Pharmacol. Res. 190 (2023), 106737.
[8] X. Gao, Y. Liu, Z. An, et al., Active components and pharmacological effects of Cornus officinalis: Literature review, Front. Pharmacol. 12 (2021), 633447.
[9] Y.H. Sung, H.K. Chang, S.E. Kim, et al., Anti-inflammatory and analgesic effects of the aqueous extract of corni fructus in murine RAW 264.7 macrophage cells, J. Med. Food 12 (2009) 788–795.
[10] L. Cao, Y. Wu, W. Li, et al., Cornus officinalis vinegar reduces body weight and attenuates hepatic steatosis in mouse model of nonalcoholic fatty liver disease, J. Food Sci. 87 (2022) 3248–3259.
[11] J. Huang, Y. Zhang, L. Dong, et al., Ethnopharmacology, phytochemistry, and pharmacology of Cornus officinalis sieb. et zucc, J. Ethnopharmacol. 213 (2018) 280–301.
[12] X. Luo, X. Bao, X. Weng, et al., The protective effect of quercetin on macrophage pyroptosis via TLR2/Myd88/NF-κB and ROS/AMPK pathway, Life Sci. 291 (2022), 120064.
[13] K. Feng, Z. Chen, P. Liu, et al., Quercetin attenuates oxidative stress-induced apoptosis via SIRT1/AMPK-mediated inhibition of ER stress in rat chondrocytes and prevents the progression of osteoarthritis in a rat model, J. Cell. Physiol. 234 (2019) 18192–18205.
[14] H. Yu, S. Yao, C. Zhou, et al., Morroniside attenuates apoptosis and pyroptosis of chondrocytes and ameliorates osteoarthritic development by inhibiting NF-κB signaling, J. Ethnopharmacol. 266 (2021), 113447.
[15] L. An, M. Zhang, Y. Lin, et al., Morroniside, a novel GATA3 binding molecule, inhibits hepatic stellate cells activation by enhancing lysosomal acid lipase expression, Phytomed. 103 (2022), 154199.
[16] T. Kisseleva, The origin of fibrogenic myofibroblasts in fibrotic liver, Hepatol. Baltim. Md 65 (2017) 1039–1043.
[17] N. Arroyo, L. Villamayor, I. Díaz, et al., GATA4 induces liver fibrosis regression by deactivating hepatic stellate cells, JCI Insight 6 (2021), e150059.
[18] T. Kisseleva, M. Cong, Y. Paik, et al., Myofibroblasts revert to an inactive phenotype during regression of liver fibrosis, Proc. Natl. Acad. Sci. U. S. A. 109 (2012) 9448–9453.
[19] X. Han, C. Ding, Y. Ning, et al., Optimizing processing technology of Cornus officinalis: Based on anti-fibrotic activity, Front. Nutr. 9 (2022), 807071.
[20] C. Ju, L. Zhu, W. Wang, et al., Cornus officinalis prior and post-processing: Regulatory effects on intestinal flora of diabetic nephropathy rats, Front. Pharmacol. 13 (2022), 1039711.
[21] L. Huang, S. Hu, M. Shao, et al., Combined Cornus officinalis and Paeonia lactiflora pall therapy alleviates rheumatoid arthritis by regulating synovial apoptosis via AMPK-mediated mitochondrial fission, Front. Pharmacol. 12 (2021), 639009.
[22] G.R. Steinberg, D.G. Hardie, New insights into activation and function of the AMPK, Nat. Rev. Mol. Cell Biol. 24 (2023) 255–272.
[23] P. Zhao, X. Sun, C. Chaggan, et al., An AMPK-caspase-6 axis controls liver damage in nonalcoholic steatohepatitis, Science 367 (2020) 652–660.
[24] X. Sun, Y. Wang, H. Zeng, et al., SIRT3 protects bovine mammary epithelial cells from heat stress damage by activating the AMPK signaling pathway, Cell Death Discov. 7 (2021), 304.
[25] A. Vassilopoulos, J.D. Pennington, T. Andresson, et al., SIRT3 deacetylates ATP synthase F1 complex proteins in response to nutrient- and exercise-induced stress, Antioxid. Redox Signal. 21 (2014) 551–564.
[26] H. Guo, Y. Ouyang, H. Yin, et al., Induction of autophagy via the ROS-dependent AMPK-mTOR pathway protects copper-induced spermatogenesis disorder, Redox Biol. 49 (2022), 102227.
[27] L. Xie, K. Wen, Q. Li, et al., CD38 deficiency protects mice from high fat diet-induced nonalcoholic fatty liver disease through activating NAD+/sirtuins signaling pathways-mediated inhibition of lipid accumulation and oxidative stress in hepatocytes, Int. J. Biol. Sci. 17 (2021) 4305–4315.
[28] B.H. Ahn, H.S. Kim, S. Song, et al., A role for the mitochondrial deacetylase Sirt3 in regulating energy homeostasis, Proc. Natl. Acad. Sci. U. S. A. 105 (2008) 14447–14452.
[29] C. Chen, J. Gu, J. Wang, et al., Physcion 8-O-β-glucopyranoside ameliorates liver fibrosis through inflammation inhibition by regulating SIRT3-mediated NF-κB P65 nuclear expression, Int. Immunopharmacol. 90 (2021), 107206.
[30] T. Zhang, J. Liu, S. Shen, et al., SIRT3 promotes lipophagy and chaperon-mediated autophagy to protect hepatocytes against lipotoxicity, Cell Death Differ. 27 (2020) 329–344.
[31] H. Dong, X. Han, M. Hao, et al., Nanodrug rescues liver fibrosis via synergistic therapy with H2O2 depletion and Saikosaponin b1 sustained release, Commun. Biol. 6 (2023), 184.
[32] L. Huang, Q. Shan, Q. Lyu, et al., MCnebula: Critical chemical classes for the classification and boost identification by visualization for untargeted LC–MS/MS data analysis, Anal. Chem. 95 (2023) 9940–9948.
[33] R. Huang, F. Guo, Y. Li, et al., Activation of AMPK by triptolide alleviates nonalcoholic fatty liver disease by improving hepatic lipid metabolism, inflammation and fibrosis, Phytomed. 92 (2021), 153739.
[34] X. Lu, W. Xuan, J. Li, et al., AMPK protects against alcohol-induced liver injury through UQCRC2 to up-regulate mitophagy, Autophagy 17 (2021) 3622–3643.
[35] T. Lan, Y. Yu, J. Zhang, et al., Cordycepin ameliorates nonalcoholic steatohepatitis by activation of the AMP-activated protein kinase signaling pathway, Hepatology 74 (2021) 686–703.
[36] T. Xin, C. Lu, SirT3 activates AMPK-related mitochondrial biogenesis and ameliorates sepsis-induced myocardial injury, Aging 12 (2020) 16224–16237.
[37] C. Chen, J. Chen, Y. Wang, et al., Ganoderma lucidum polysaccharide inhibits HSC activation and liver fibrosis via targeting inflammation, apoptosis, cell cycle, and ECM-receptor interaction mediated by TGF-β/Smad signaling, Phytomedicine 110 (2023), 154626.
[38] G. Szabo, J. Petrasek, Inflammasome activation and function in liver disease, Nat. Rev. Gastroenterol. Hepatol. 12 (2015) 387–400.
[39] Y. Yan, S. Mukherjee, K.G. Harikumar, et al., Structure of an AMPK complex in an inactive, ATP-bound state, Science 373 (2021) 413–419.
[40] Y. Deng, M. Xie, Q. Li, et al., Targeting mitochondria-inflammation circuit by β-hydroxybutyrate mitigates HFpEF, Circ. Res. 128 (2021) 232–245.